Ion Pairing in Aqueous Lithium Salt Solutions with Monovalent and Divalent Counter-Anions

Eva Pluhařová, Philip E. Mason, and Pavel Jungwirth**

Institute of Organic Chemistry and Biochemistry, Academy of Sciences of the Czech Republic, Flemingovo nám. 2, 16610 Prague 6, Czech Republic

*Corresponding authors: philip.mason@uochb.cas.cz and pavel.jungwirth@uochb.cas.cz

KEYWORDS: lithium, aqueous solution, neutron scattering, molecular dynamics, polarizability

Abstract

Molecular dynamics simulations of concentrated aqueous solutions of LiCl and Li_2SO_4 were conducted in order to provide molecular insight to recent neutron scattering data. The structures predicted from the molecular dynamics simulations using standard non-polarizable force fields provided a very poor fit to the experiment, therefore, refinement was needed. The electronic polarizability of the medium was effectively accounted for by implementing the electronic continuum correction, which practically means rescaling the ionic charges. Consistent with previous studies we found that this approach in each case provided a significantly improved fit to the experimental data, which was further enhanced by slightly adjusting the radius of the

lithium ion. The polarization effect was particularly pronounced in the Li_2SO_4 solution where the ions in the non-polarizable simulations tended to cluster unphysically. With the above alterations the employed force field displayed an excellent fit to the neutron scattering data and provided useful interpretative framework for the experimental measurements. At the same time, the present study underlines the importance of solvent polarization effects in hydration of ions with high charge density.

Introduction

The lithium ion has many important technological applications. The most significant of these are the Li-ion polymer batteries[1,2] which power almost all of the modern portable electronic devices. Other industrial applications include the use of lithium stearates for grease production,[3] metallic lithium for high strength and low weight alloys,[4] and lithium carbonate in the glass and porcelain industry and psychiatric medicine.[5] Further, the lithium ion in aqueous solution has also been a controversial subject in physical chemistry, primarily due to lack of a consistent hydration picture obtained from experimental and simulations techniques.[6,7] From the experimental side this is primarily because of technical challenges in acquiring or interpreting the data relevant to the hydration of the lithium ion. X-ray scattering is of limited use when applied to aqueous solutions of lithium salts due to the low number of electrons in the lithium ion.[8,9] Arguably the best method for the determination of hydration structure of the lithium ion is neutron scattering,[10-18] specifically the technique of neutron diffraction with isotopic substitution (NDIS) with the $^{6/7}$Li labeling.[17] However, this measurement suffers from an additional complication since ^{6}Li is a strong absorber of neutrons, but ^{7}Li is not. Nevertheless, since the earlier NDIS measurements there has been a large increase in the sensitivity and stability of

neutron detectors.[19] Also, faster computers allow for a more sophisticated treatment of the multiple scattering and absorption corrections that must be performed on the neutron scattering data in order to obtain a first order difference signal that accurately reflects the lithium ion hydration.[20]

Empirical force fields employed in classical molecular dynamics simulations suffer from deficiencies when used to study the hydration of the lithium ion. Li^+ has the highest charge density of all the alkali metal ions. While the lithium ion is practically non-polarizable, the high charge density of the ion effects the charge distribution on the surrounding water molecules and it can also lead to charge transfer from water to the metal ion. Ab initio molecular dynamics (AIMD) methods can in principle yield useful information about the system,[7,21,22] however, they may become prohibitively computationally demanding for obtaining converged distribution functions in concentrated solutions that could be directly compared to neutron scattering data. Ab initio studies of Li^+ in the aqueous bulk or clusters yield a coordination number for the lithium ion of ~4,[21,23] while classical molecular dynamics (MD) simulations (with non-polarizable potentials) give a value of ~5-7. [8,24-26] Structural experiments, which almost always examine concentrated solutions, have previously yielded coordination numbers between 4 and 6.[10,11] Most ab initio studies yield a peak in the radial distribution functions corresponding to oxygen atoms in the first hydration shell of Li^+ at ~2.0 Å,[21,23] while MD studies yield values around 2.1 Å.[8,24-26] While this may seem to be a small difference, the fit between the experimental results and the MD simulations is very sensitive to the actual radius of the lithium ion, as we show later in this paper.

The use of a polarizable force field should provide a more realistic answer than that from standard non-polarizable simulations, however, they are also more costly to run. The effects of

including the lithium polarizability would be negligible due to the low polarizability of Li^+, while the electronic polarization of water molecules by the ions may significantly influence the behavior of these solutions. A simple and effective way of accounting for the electronic polarizability of water in ionic solutions is by scaling the ionic charges by $1/\sqrt{\varepsilon_{el}}$, where ε_{el} = 1.78 is the electronic part of the static relative permittivity of water (i.e., yielding a scaling factor of 0.75).[27-30] Consistent with our earlier work, which resulted in a significantly improved agreement between the simulation and experimental results for other aqueous salt solutions, we further refer to this approach as the electronic continuum correction (ECC).[31,32,33]

The primary focus of the present paper is to quantitatively interpret and provide molecular insight to the most recent neutron scattering results[34] of LiCl and Li_2SO_4 aqueous solutions by means of MD simulations. To meet this challenge we had to go beyond the widely used non-polarizable force fields which yielded significant deviations from the experimental data. In order to obtain a better fit to the experiment we employed the ECC approach and also further refined the radius of the lithium ion.

Methods

Classical molecular dynamics simulations were performed for aqueous solutions of 1.5 m Li_2SO_4 and 3.0 m LiCl. The first system consisted of 72 Li^+ and 36 SO_4^{2-} and 1333 water molecules in a cubic box with a length of 34.55 Å giving the experimental number density of 0.103 atoms/Å^3. The 3.0 m LiCl solution contains 72 Li^+, 72 Cl^-, and 1333 water molecules in a cubic box with a length of 34.789 Å giving the experimental number density of 0.0984 atoms/Å^3. The OPLS force field was used initially for the lithium ion, while the sulfate force field was

taken from our recent study on Na_2SO_4.[33] The water model employed was SPC/E.[35] Other ionic force fields also in combination with the TIP4P[36] water model were tested as well, with results presented in the Supporting Information (SI).

For both systems we used either full ionic charges or the ECC approach (which effectively means scaling the ionic charges by a factor of 0.75).[27-30] Since the size of lithium ion was parameterized together with the full charge model, after scaling the charges we also refined the radius resulting in a slightly smaller Li^+. In total, four simulations were thus run for each system (i.e., full or scaled ionic charges with larger or smaller sized lithium ions). The details of the force field parameters are summarized in Table 1.

For each system we collected 30 ns trajectories with a 1 fs time step employing the Gromacs software.[37] Simulations were performed at constant volume and constant temperature of 300 K maintained by the canonical sampling through velocity rescaling (CSVR) thermostat[38] with a time constant of 0.5 ps. The internal geometry of water molecules was kept rigid using the Settle algorithm.[39] 3D periodic boundary conditions were applied. Short range electrostatic and van der Waals interactions were truncated at 1.2 nm, with the long-range electrostatic interactions being treated by the particle mesh Ewald method.[40]

The radial distribution functions between lithium and all other atoms were calculated from the above simulations and used to emulate the $^{6/7}$Li substitution NDIS measurement. In each case the first order difference function ($^{Cl}\Delta G_{Li}(r)$ or $^{SO4}\Delta G_{Li}(r)$) is a sum of weighted radial distribution functions. Specifically for the 3m LiCl and 1.5 m Li_2SO_4 in D_2O these functions are:

$$^{SO4}\Delta G_{Li}(r) = 5.68\, g_{LiD}(r) + 2.74\, g_{LiO}(r) + 0.033\, g_{LiS}(r) - 0.005\, g_{LiLi}(r) - 8.45 \quad (1)$$

$$^{Cl}\Delta G_{Li}(r) = 5.98\, g_{LiD}(r) + 2.60\, g_{LiO}(r) + 0.23\, g_{LiCl}(r) - 0.005\, g_{LiLi}(r) - 8.81 \quad (2)$$

In each case the prefactors for the radial distribution functions g(r) are calculated using the formula $c_{\mathrm{Li}}c_{\mathrm{x}}\Delta b_{\mathrm{Li}}b_{\mathrm{x}}$ where c is the atomic concentration of that nuclei, b is the average coherent neutron scattering length of that nuclei, and Δb_{Li} is the difference in the coherent scattering lengths of ^{7}Li and ^{6}Li (the last number on the right in both equations is the sum of the prefactors).

As the measurements were originally made in Q-space, this representation is a more direct format for comparing the experimental and modeling data. The calculated real space functions ($^{Cl}\Delta G_{Li}(r)$ and $^{SO4}\Delta G_{Li}(r)$) were, therefore, back Fourier transformed to yield the first order difference functions in Q-space:

$$^{SO4}\Delta S_{Li}(Q) = 5.68\, S_{LiD}(Q) + 2.74\, S_{LiO}(Q) + 0.033\, S_{LiS}(Q) - 0.005\, S_{LiLi}(Q) - 8.45 \quad (3)$$

$$^{Cl}\Delta S_{Li}(Q) = 5.98\, S_{LiD}(Q) + 2.60\, S_{LiO}(Q) + 0.23\, S_{LiCl}(Q) - 0.005\, S_{LiLi}(Q) - 8.81 \quad (4)$$

This back transformed functions, while in principle containing the same information as the real space functions, are useful by emphasizing different parts of the data.

Results and Discussion

Molecular dynamics has proven to be an excellent interpretive tool for neutron scattering data[41-43] and by virtue of comparison with the experimental data we can also determine whether characteristics observed in the simulations are physically realistic or not.[31,44,45] For lithium salt

solutions standard force fields tend to provide a poor match to the experiment. This is exemplified in Figure 1a, which depicts a snapshot from MD simulation of 1.5 m Li_2SO_4 using the OPLS force field. Despite being well below the solubility limit, the ions actually cluster together and effectively fall out of the solution. Other widely used non-polarizable force fields were also tested (for details see SI), but provided similarly disappointing results. In order to obtain a better match with experimental reality, we first effectively included solvent polarization effects via the ECC approach, i.e., by rescaling the ionic charges. This qualitatively improved the behavior of the system as demonstrated in Figure 1b showing now a regular behavior of the 1.5 M Li_2SO_4 solution. Quantitatively, the description of the systems could be further improved by slightly adjusting the radius of the lithium ion (for comparison to NDIS data see below), which was originally parameterized without any account for polarizability.

For each of the two studied solutions (i.e., 1.5 m Li_2SO_4 and 3.0 m LiCl) we have thus performed four simulations starting with the original non-polarizable force field and applying the ECC correction or reducing the size of the lithium ion or both. The effects of changing the ionic charges from full to ECC ones on the lithium-sulfate interactions can be seen in the radial distribution functions $g_{LiS}(r)$ (Figure 2). For both larger and smaller lithium radii, lowering the charge on the ions reduces the amount of ion pairing, i.e., the height of the first peak in the radial distribution function (see also Table 2). Analogous but less pronounced changes were observed with including the ECC correction in the simulations of LiCl solutions (Figure 2), since in the first place none of the LiCl trajectories produced strong ion pairing and clustering such as that found in the full charge simulations of Li_2SO_4.

By reducing the lithium radius the ion-pairing peaks in $g_{LiCl}(r)$ and $g_{LiS}(r)$ move to slightly smaller interionic distances (Figure 2). Furthermore, in the Li_2SO_4 solution the ion

pairing peak in the function $g_{LiS}(r)$ at ~ 3 Å changes from being mostly bimodal to primarily monomodal. This change in character can be most seen clearly in the density maps of Li^+ around SO_4^{2-} (Figure 3). The monomodal behavior with the smaller lithium is mostly due to the linear (monodentate) S-O-Li^+ interaction, whereas the bimodal character with the larger lithium is due to populations of both mondentate and bidentate (i.e., with the metal ion bridging two oxygens) lithium association with sulfate.

The composition of the first hydration shells of the lithium ion from all the simulations is presented in Table 2. In all cases the ECC simulations display less ion pairing than their full charges counterparts, which results in a larger number of water molecules in the Li^+ hydration shell. The effect of changing the Li^+ size has an influence on the hydration shells in all of these solutions. In all cases the smaller lithium ion has a total coordination number (i.e., number of atoms in direct contact with the ion) of four, while for larger Li^+ this number somewhat increases and becomes more variable (Table 2).

In order to compare to experiment the first order difference functions ${}^{Cl}\Delta G_{Li}(r)$ and ${}^{SO4}\Delta G_{Li}(r)$ (see Eqs. 1-2) previously determined via neutron scattering[34] were calculated from the molecular dynamics simulations (Figures 4 and 5 for the Li_2SO_4 and LiCl solutions). The solution structure of lithium always displays several common features in these functions.[11,21,24] The first peak at ~2 Å is mostly due to oxygen atoms solvating the ion, while the second peak at 2.5 Å is mostly due to the hydrogen atoms of water molecules solvating the ion (Figures 4 and 5). This general form is found in all the simulations in this study, and is broadly consistent with previous experimental and theoretical modeling studies.[10,11,15,46] Simulations with full charges provide an incorrect aspect ratio between these two peaks, particularly for the Li_2SO_4 solution.

This is due to excessive ion pairing which exemplifies the first peak (which has contributions both from lithium-water oxygen and lithium-sulfate oxygen correlations) over the second one (which is dominantly due to lithium-water hydrogen interactions), see Figure 4. By reducing ion pairing and clustering the ECC method brings the intensities of the two peaks into much better agreement with experiment. In addition, for all of the simulations with the larger Li^+ ion, the first and second peaks at 2 and 2.5 Å mismatched those found in the experimental data by ~0.1 Å. The smaller lithium radius was, therefore, chosen based on the assumption that a linear reduction in the radius would lead to a linear shift in the peak position. This assumption proved to be valid in all the studied cases and allowed for a good fit to the experimental peak positions. Qualitatively, the improvements by including the ECC method for implementing polarizability and adjusting the lithium radius are seen directly from the plots in Figure 4. Quantitatively, this is demonstrated in Table 3, which provides root mean square deviations between the experimental and calculated first order difference functions from Figure 4 for all the simulations of both systems.

The comparison of the MD results and previously measured experimental data[34] (which have been splined here to reduce the residual ringing errors) can be performed either in *r*-space (Figures 4 and 5) or in Q-space (Figures 6 and 7 for Li_2SO_4 and LiCl). Both comparisons in principle contain the same information, however, they emphasize different aspects of the structure of the solution. While *r*-space may be a more intuitive representation for viewing the data, in many ways it is more satisfactory if the comparison can be performed in Q-space, as this is more closely related to what is directly measured in the experiment. It is, therefore, necessary to have a rough understanding of the relationship between *r*- and Q-space data. The general relationship between *r* and Q space is analogous to that between wavelength and frequency.

Sharper features at lower *r* tend to be expressed as longer wavelength features in Q and are particularly visible at higher Q values. The wavelength of these features corresponds to the peak position in *r*-space. The first two peaks in *r*-space at roughly 2 and 2.5 Å effectively produce two sine-type waves of different frequencies in Q-space. The fact that the peak positions for the two peaks do not match for the larger lithium ion translates into a phase shift in the data at higher Q in the Q-space. Figures 6 and 7 thus exemplify that even a very small peak shift of 0.1 Å can turn a phase disagreement between the MD and experimental data into an excellent agreement, provided the ECC method is applied as well.

The highly damped, high frequency elements in Q-space correspond to longer range features in *r*-space. Most of the features in *r*-space past the first hydration shell are seen in the lower range Q-space data (0-5 $Å^{-1}$). This can most easily be seen in the comparison of the ECC and full charge simulations of Li_2SO_4 where the latter simulation has significantly more longer range structure than the former one, yielding an incorrect signal in the lower Q region (Figure 6). In Li_2SO_4, as well as LiCl solutions the ECC charges thus provide a better match to the lower Q region than the full charge simulation.

Taken together the present results show that the ECC simulations with the smaller lithium ion provide the best fit to the experimental data. Further, the comparisons give a measure of how sensitive the results are to changes in simulation parameters, and if such changes could be distinguished by the experimental data. In the present case, experimental data can easily decide that effectively polarizable simulations with the ECC charges provide a significantly better fit to the experimental data than the non-polarizable simulations with full charges and can also differentiate the effect of a change of the order of 0.1 Å in the radius of the lithium ion.

Conclusions

In the present study, molecular dynamic simulations of aqueous solutions of 3m LiCl and 1.5m Li_2SO_4 were carried out and compared to the most recent neutron scattering data.[34] These experimental data are particularly informative as the NDIS substitution was performed directly on the lithium nucleus rather than the hydrogen, providing a more direct insight into the hydration of the lithium ion. Initial MD simulations with standard non-polarizable force fields displayed clear inadequacies in terms of excessive ion pairing and clustering that limited their use as interpretive tools. Modifications of the interaction potentials were, therefore, required for obtaining a good fit and providing interpretation to the experimental data. In the MD simulations both the effect of incorporating the electronic polarizability of the medium and adjusting the size of the lithium ion were examined. Electronic polarizability of the solvent was implemented in an effective way via scaling of the ionic charges.[27] For both the LiCl and Li_2SO_4 solutions this electronic continuum correction provided a significantly improved fit to experimental neutron scattering data compared to the full charge simulations. This was particularly visible in the Li_2SO_4 solutions where within the full charge simulation the ions strongly clustered and effectively fell out of the solution (even though the simulation was performed well below the solubility limit of Li_2SO_4), while the ECC simulation provided a regular solution with a realistic degree of ion pairing. Once the electronic polarization of the solvent was effectively accounted for, a small adjustment (decrease) of the radius of the lithium ion allowed for obtaining an excellent fit to the neutron scattering data. These simulation results also suggest that the coordination number of lithium in these solutions is ~4 for both the sulfate and chloride counter-anions. In general, the present work shows that for accurate description of aqueous salt solutions

containing ions with high charge density, such as lithium and sulfate, electronic polarization effects of the solvent need to be included at least in an effective way.

Acknowledgment

Support from the Czech Ministry of Education (grant no. LH12001) is gratefully acknowledged. P.J. thanks the Academy of Sciences for the Praemium Academie award. P.E.M. thanks Henry Fischer and the D4C staff of the Institute Laue Langevin for their help. E. P. acknowledges support from the International Max Planck Research School on Dynamical Processes in Atoms, Molecules, and Solids. Access to computing and storage facilities MetaCentrum, provided under the program "Projects of Large Infrastructure for Research, Development, and Innovations" (LM2010005) is acknowledged.

Supporting Information provides further computational details including force field parameters of the ions. This material is available free of charge via the Internet at http://pubs.acs.org.

Tables

Table 1. Force field parameters of ions employed in simulations of Li_2SO_4 and LiCl aqueous solutions.

	σ (Å)	ε (kJ/mol)	Charge (full/ECC)
Larger Li^+	2.126	0.07647	+1.0 / +0.75
Smaller Li^+	1.80	0.07647	+1.0 / +0.75
S	3.550	1.046	+2.0 / +1.50
O (of sulfate)	3.150	0.8368	-1.0 / -0.75
Cl	4.417	0.4928	-1.0 / -0.75

Table 2. The composition of the first hydration shells of Li^+ for all the MD simulations. In each case, the number of species (i.e., water oxygen, sulfate oxygen, or chloride) in direct contact with the lithium ion is evaluated by integrating up to the first minimum in radial distribution function. The percentage of each species in the hydration shell is shown in parenthesis.

		Full Charges		ECC charges	
		Larger Lithium	Smaller Lithium	Larger Lithium	Smaller Lithium
LiCl	Ow	4.3 (95 %)	3.8 (94 %)	4.1 (93 %)	3.9 (97 %)
	Cl	0.34 (5 %)	0.22 (5 %)	0.30 (7 %)	0.12 (3 %)
	Total	4.7	4.0	4.4	4.0
Li_2SO_4	Ow	1.8 (61 %)	2.4 (60 %)	3.9 (90 %)	3.7 (93 %)
	Os	2.8 (39 %)	1.6 (40 %)	0.43 (10 %)	0.27 (7 %)
	Total	4.5	4.0	4.3	4.0

Table 3. Root mean square deviations between the experimental and calculated weighted first order difference functions $\Delta G_{Li}(r) \cdot r^2$ in the range 1.5-6 Å for all the performed simulations of Li_2SO_4 and LiCl aqueous solutions.

	Full Charges		ECC charges	
	Larger Lithium	Smaller Lithium	Larger Lithium	Smaller Lithium
LiCl	2.5×10^{-3}	2.2×10^{-3}	2.3×10^{-3}	1.4×10^{-3}
Li_2SO_4	3.0×10^{-3}	1.9×10^{-3}	2.2×10^{-3}	1.0×10^{-3}

Figure Captions

Figure 1. Snapshots from the simulations of a 1.5m Li_2SO_4 solution with full charges on the left, where the ions strongly aggregate and ECC charges on the right, where the ions are more homogeneously distributed. Water molecules are shown in stick representation. All simulation images were created using VMD.[47]

Figure 2 The lithium-chloride and lithium-sulfate sulphur radial distribution functions for the eight simulations in this study. In each plot in black is the full charges simulation and in red is the ECC charges simulation. Left - the function $g_{LiCl}(r)$ for 3m LiCl solutions and right - the function $g_{LiS}(r)$ for the 1.5 m Li_2SO_4 solutions. In each case blue vertical lines have been added to highlight the peak shifts that occur when the different lithium sizes are used. Note the change in the contact ion pair peak in $g_{LiS}(r)$ from somewhat bimodal to monomodal as the size of the lithium ion is decreased.

Figure 3 Density maps of lithium around sulfate as calculated from the MD simulations of larger (purple) and smaller lithium ions (cyan), both with ECC charges.

Figure 4 First order difference functions in the *r*-space for Li_2SO_4 solutions. Black - experimentally measured function ${}^{SO4}\Delta G_{Li}(r)$ (in each case the non-physical termination errors from the Fourier transformation are shown in grey).[34] Red - the same function calculated from MD simulations. Left - full charges and right - ECC charges. Upper plots - larger lithium ion and lower plots - smaller lithium ion.

Figure 5 First order difference functions in the *r*-space for LiCl solutions. Black - experimentally measured function ${}^{Cl}\Delta G_{Li}(r)$ (in each case the non-physical termination errors

from the Fourier transformation are shown in grey).[34] Red - the same function calculated from MD simulations. Left - full charges and right - ECC charges. Upper plots - larger lithium ion and lower plots - smaller lithium ion.

Figure 6 First order difference functions in the Q-space for Li_2SO_4 solutions. Black - experimentally measured function ${}^{SO4}\Delta S_{Li}(Q)$.[34] Red - the same function calculated from MD simulations. Left - full charges and right - ECC charges. Upper plots - larger lithium ion and lower plots - smaller lithium ion.

Figure 7 First order difference functions in the Q-space for LiCl solutions. Black - experimentally measured NDIS function ${}^{Cl}\Delta S_{Li}(Q)$.[34] Red - the same function calculated from MD simulations. Left - full charges and right - ECC charges. Upper plots - larger lithium ion and lower plots - smaller lithium ion.

Figures

Figure 1

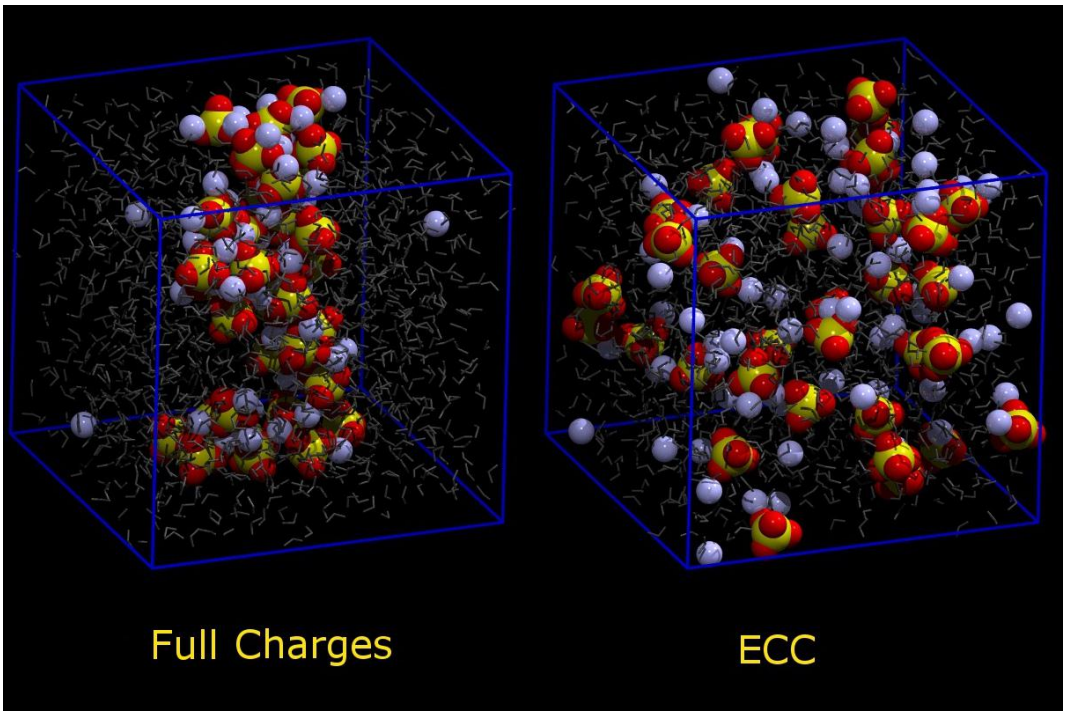

Figure 2

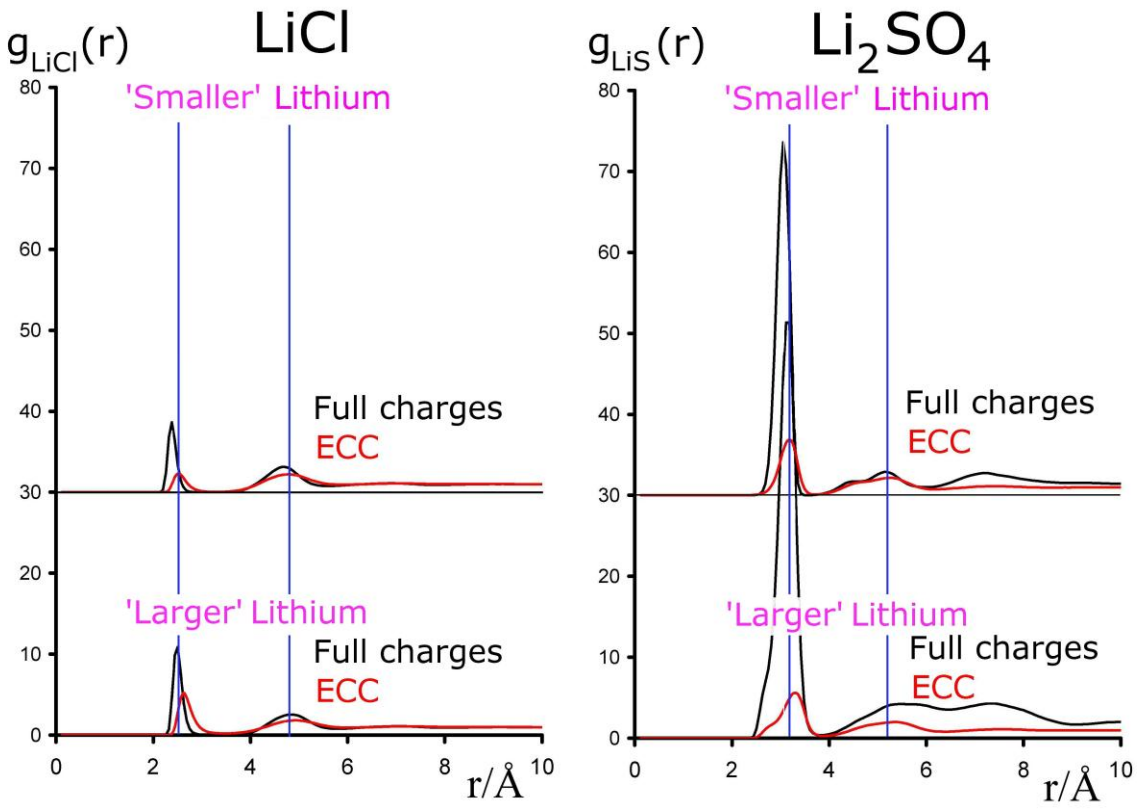
LiCl
$g_{LiCl}(r)$
'Smaller' Lithium
Full charges
ECC
'Larger' Lithium
Full charges
ECC
r/Å
Li_2SO_4
$g_{LiS}(r)$
'Smaller' Lithium
Full charges
ECC
'Larger' Lithium
Full charges
ECC
r/Å

Figure 3

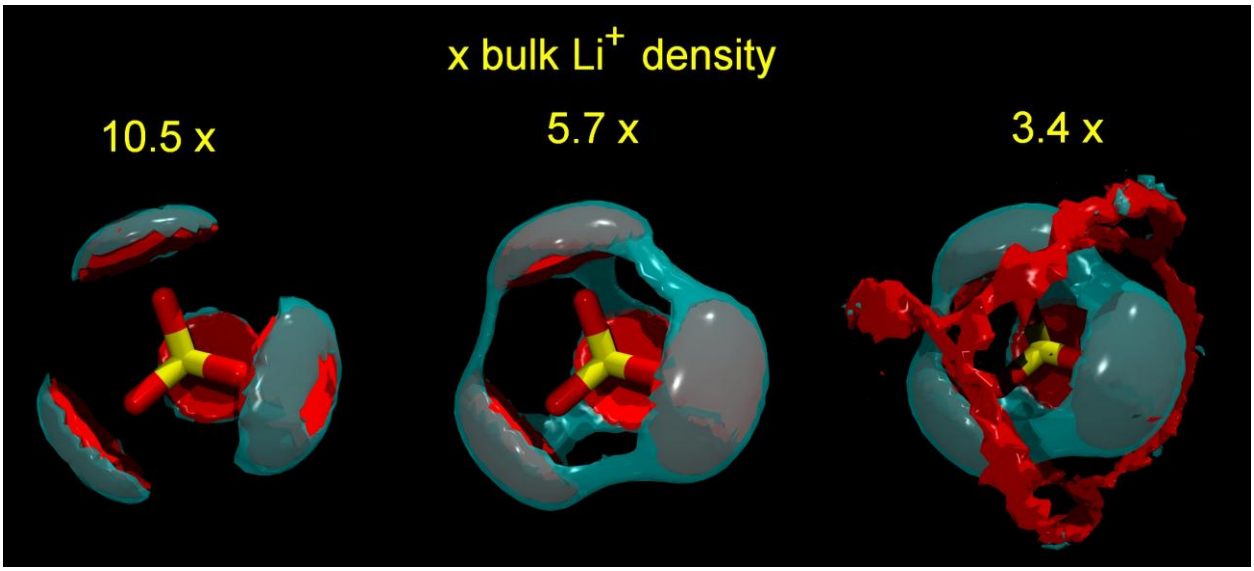

Figure 4

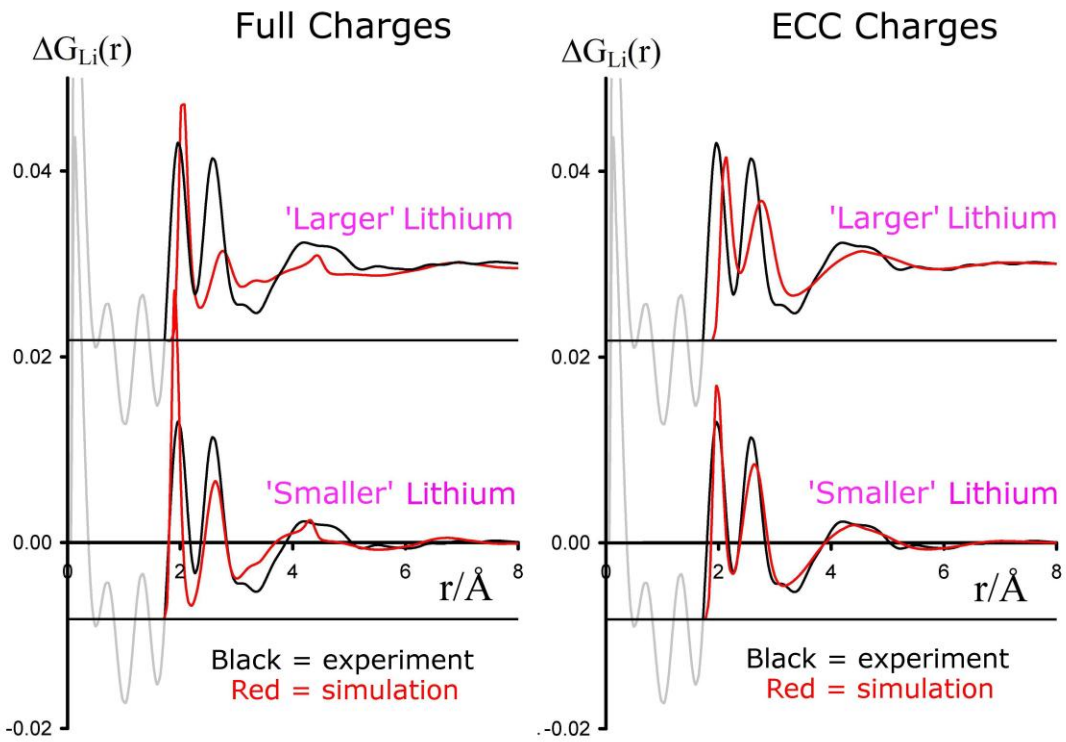
Full Charges
ECC Charges
ΔG_Li(r)
0.04
0.02
0.00
-0.02
'Larger' Lithium
'Smaller' Lithium
0
2
4
6
8
r/Å
Black = experiment
Red = simulation

Figure 5

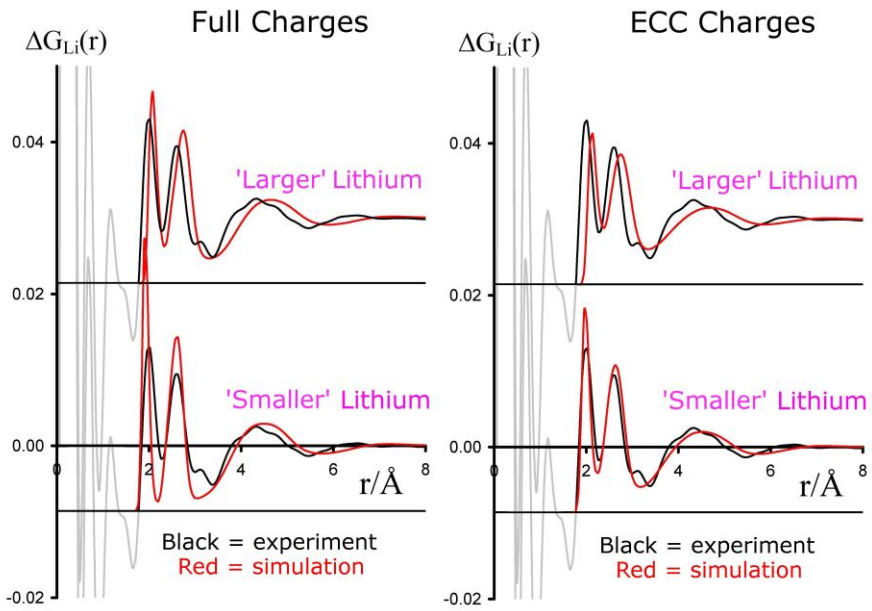
Full Charges
ECC Charges
ΔG_Li(r)
0.04
0.02
0.00
-0.02
'Larger' Lithium
'Smaller' Lithium
0
2
4
6
8
r/Å
Black = experiment
Red = simulation

Figure 6

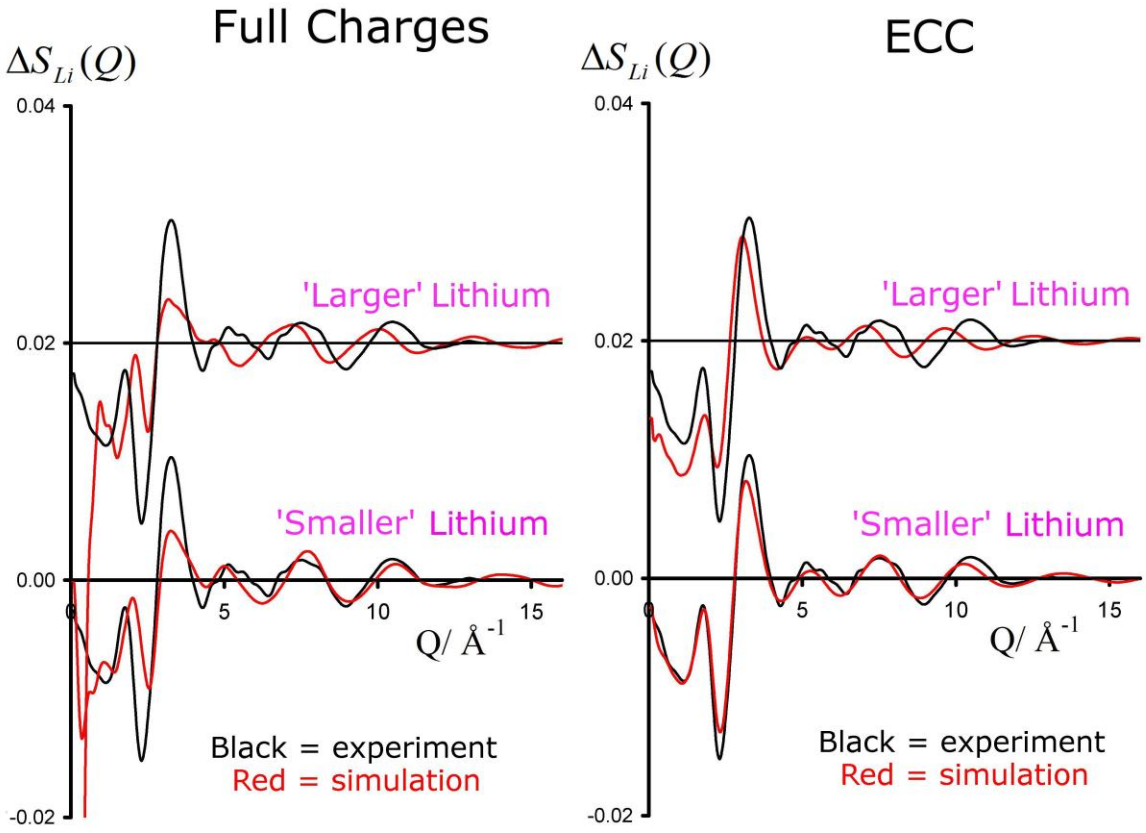
Full Charges
ECC
$\Delta S_{Li}(Q)$
0.04
0.02
0.00
-0.02
'Larger' Lithium
'Smaller' Lithium
0
5
10
15
Q/ Å^{-1}
Black = experiment
Red = simulation

Figure 7

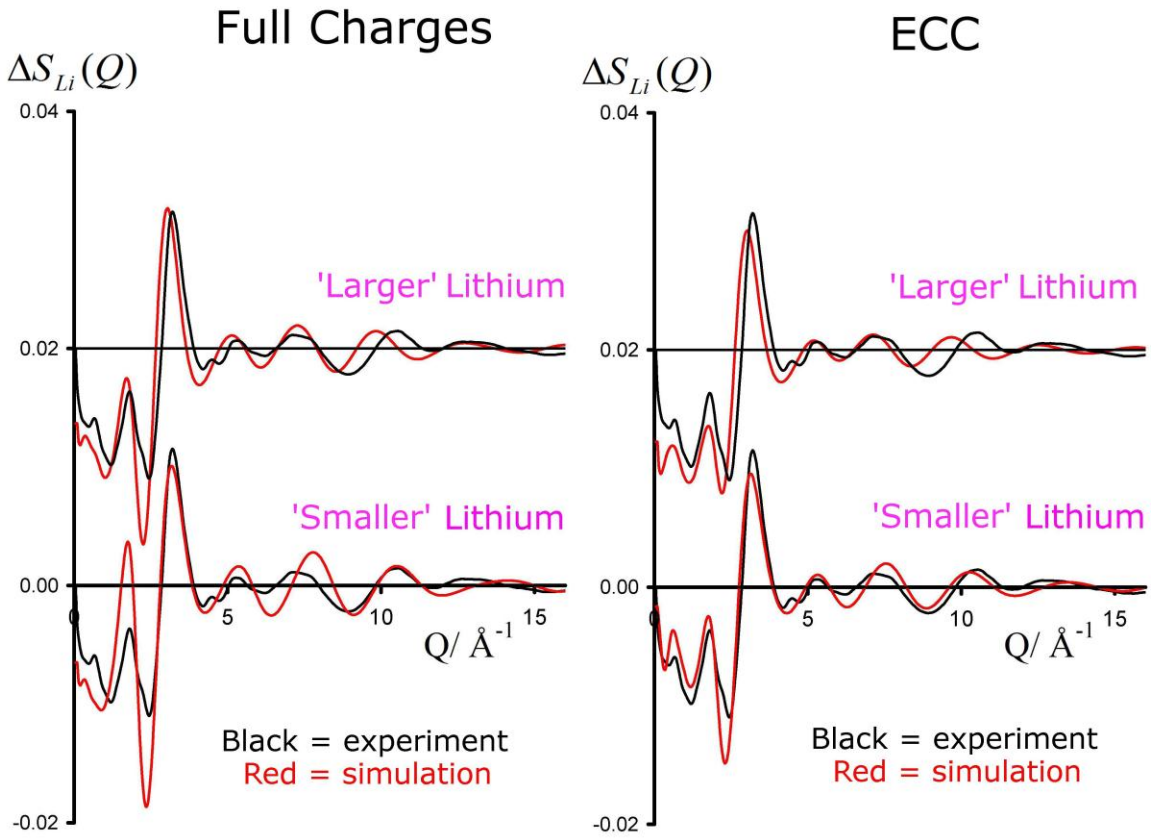
Full Charges
ECC
$\Delta S_{Li}(Q)$
0.04
0.02
0.00
-0.02
'Larger' Lithium
'Smaller' Lithium
0
5
10
15
Q/ Å^{-1}
Black = experiment
Red = simulation

TOC Graphics

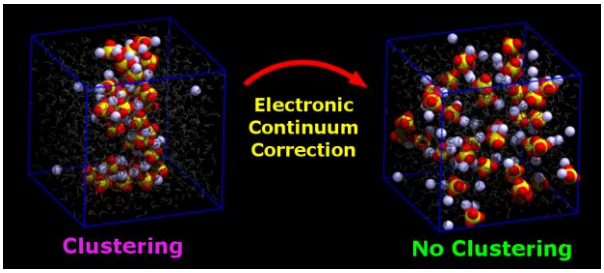

References

1. Whittingham, M. S., Lithium Batteries and Cathode Materials. *Chem. Rev.* **2004,** *104*, 4271-4301.

2. Tarascon, J. M.; Armand, M., Issues and Challenges Facing Rechargeable Lithium Batteries. *Nature* **2001,** *414*, 359-367.

3. Delgado, M. A.; Sanchez, M. C.; Valencia, C.; Franco, J. M.; Gallegos, C., Relationship Among Microstructure, Rheology and Processing of a Lithium Lubricating Grease. *Chem. Eng. Res. Des.* **2005,** *83*, 1085-1092.

4. Polmear, I. J., Recent Developments in Light Alloys. *Mat. Trans. JIM* **1996,** *37*, 12-31.

5. Mahler, J.; Persson, I., A Study of the Hydration of the Alkali Metal Ions in Aqueous Solution. *Inorg. Chem.* **2012,** *51*, 425-438.

6. Varma, S.; Rempe, S. B., Coordination Numbers of Alkali Metal Ions in Aqueous Solutions. *Biophys. Chem.* **2006,** *124*, 192-199.

7. San-Roman, M.; Carrillo-Tripp, M.; Saint-Martin, H.; Hernandez-Cobos, J.; Ortega-Blake, I., A Theoretical Study of the Hydration of Li+ by Monte Carlo Simulations with Refined Ab Initio Based Model Potentials. *Theor. Chem. Acc.* **2006,** *115*, 177-189.

8. Harsanyi, I.; Pusztai, L., Hydration Structure in Concentrated Aqueous Lithium Chloride Solutions: A Reverse Monte Carlo Based Combination of Molecular Dynamics Simulations and Diffraction Data. *J. Chem. Phys.* **2012,** *137*, 204503.

9. Bouazizi, S.; Nasr, S., Local Order in Aqueous Lithium Chloride Solutions as Studied by X-ray Scattering and Molecular Dynamics Simulations. *J. Mol. Struct.* **2007,** *837*, 206-213.

10. Newsome, J. R.; Neilson, G. W.; Enderby, J. E., Lithium Ions in Aqueous Solution. *J. Phys. C-Solid State Phys.* **1980,** *13*, L923-L926.

11. Copestake, A. P.; Neilson, G. W.; Enderby, J. E., The Structure of a Highly Concentrated Aqueous Solution of Lithium Chloride. *J. Phys. C-Solid State Phys.* **1985,** *18*, 4211-4216.

12. Vandermaarel, J. R. C.; Powell, D. H.; Jawahier, A. K.; Leytezuiderweg, L. H.; Neilson, G. W.; Bellissent-Funel, M. C., On the Structure and Dynamics of Lithium Counterions in Polyelectrolyte Solutions - A Nuclear Magnetic Resonance and Neutron Scattering Study. *J. Chem. Phys.* **1989,** *90*, 6709-6715.

13. Tromp, R. H.; Neilson, G. W.; Soper, A. K., Water Structure in Concentrated Lithium Chloride Solutions. *J. Chem. Phys.* **1992,** *96*, 8460-8469.

14. Adya, A. K.; Neilson, G. W.; Okada, I.; Okazaki, S., The Determination of the Radial Distribution Functions gLi-Li(R), gLLi-O(R), and gLi-N(R) in Molten Lithium Nitrate from Neutron Diffraction. *Mol. Phys.* **1993,** *79*, 1327-1350.

15. Ansell, S.; DupuyPhilon, J.; Jal, J. F.; Neilson, G. W., Ionic Structure in the Aqueous Electrolyte Glass LiCl Center dot 4D(2)O. *J. Phys.-Condens. Mat.* **1997,** *9*, 8835-8847.

16. Ansell, S.; Neilson, G. W., Anion-Anion Pairing in Concentrated Aqueous Lithium Chloride Solution. *J. Chem. Phys.* **2000,** *112*, 3942-3944.

17. Howell, I.; Neilson, G. W., Li+ Hydration in Concentrated Aqueous Solution. *J. Phys.-Condens. Mat.* **1996,** *8*, 4455-4463.

18. Ansell, S.; Barnes, A. C.; Mason, P. E.; Neilson, G. W.; Ramos, S., X-ray and Neutron Scattering Studies of the Hydration Structure of Alkali Ions in Concentrated Aqueous Solutions. *Biophys. Chem.* **2006,** *124*, 171-179.

19. Fischer, H. E.; Cuello, G. J.; Palleau, P.; Feltin, D.; Barnes, A. C.; Badyal, Y. S.; Simonson, J. M., D4c: A Very High Precision Diffractometer for Disordered Materials. *Appl. Phys. A - Mat. Sci. Proces.* **2002,** *74*, S160-S162.

20. Dawidowski, J.; Cuello, G. J.; *Experimental corrections in neutron diffraction of ambient water using H/D isotopic substitution*, Proceedings of the 5th European Conference on Neutron Scattering (ECNS), Prague, Czech Republic, 2011.

21. Petit, L.; Vuilleumier, R.; Maldivi, P.; Adamo, C., Ab Initio Molecular Dynamics Study of a Highly Concentrated LiCl Aqueous Solution. *J. Chem. Theor. Comput.* **2008,** *4*, 1040-1048.

22. Ohrn, A.; Karlstrom, G., A Combined Quantum Chemical Statistical Mechanical Simulation of the Hydration of Li+, Na+, F-, and Cl. *J. Phys. Chem. B* **2004,** *108*, 8452-8459.

23. Rempe, S. B.; Pratt, L. R.; Hummer, G.; Kress, J. D.; Martin, R. L.; Redondo, A., The Hydration Number of Li(+) in Liquid Water. *J. Am. Chem. Soc.* **2000,** *122*, 966-967.

24. Harsanyi, I.; Pusztai, L., On the Structure of Aqueous LiCl Solutions. *J. Chem. Phys.* **2005,** *122*, 124512.

25. Egorov, A. V.; Komolkin, A. V.; Chizhik, V. I., Influence of Temperature on the Microstructure of the Lithium-Ion Hydration Shell. A Molecular Dynamics Description. *J.Mol. Liq.* **2000,** *89*, 47-55.

26. Egorov, A. V.; Komolkin, A. V.; Chizhik, V. I.; Yushmanov, P. V.; Lyubartsev, A. P.; Laaksonen, A., Temperature and Concentration Effects on Li+-ion Hydration. A Molecular Dynamics Simulation Study. *J. Phys. Chem. B* **2003,** *107*, 3234-3242.

27. Leontyev, I.; Stuchebrukhov, A., Accounting for Electronic Polarization in Non-Polarizable Force Fields. *Phys. Chem. Chem. Phys.* **2011,** *13*, 2613-2626.

28. Leontyev, I. V.; Stuchebrukhov, A. A., Electronic Continuum Model for Molecular Dynamics Simulations of Biological Molecules. *J. Chem. Theor. Comput.* **2010,** *6*, 1498-1508.

29. Leontyev, I. V.; Stuchebrukhov, A. A., Electronic Polarizability and the Effective Pair Potentials of Water. *J. Chem. Theor. Comput.* **2010,** *6*, 3153-3161.

30. Leontyev, I. V.; Stuchebrukhov, A. A., Electronic Continuum Model for Molecular Dynamics Simulations. *J. Chem. Phys.* **2009,** *130*, 085102.

31. Mason, P. E.; Wernersson, E.; Jungwirth, P., Accurate Description of Aqueous Carbonate Ions: An Effective Polarization Model Verified by Neutron Scattering. *J. Phys. Chem. B* **2012,** *116*, 8145-8153.

32. Vazdar, M.; Jungwirth, P.; Mason, P. E., Aqueous Guanidinium–Carbonate Interactions by Molecular Dynamics and Neutron Scattering: Relevance to Ion–Protein Interactions. *J. Phys. Chem. B* **2012,** *117*, 1844-1848.

33. Wernersson, E.; Jungwirth, P., Effect of Water Polarizability on the Properties of Solutions of Polyvalent Ions: Simulations of Aqueous Sodium Sulfate with Different Force Fields. *J. Chem. Theor. Comput.* **2010,** *6*, 3233-3240.

34. Ansell, S.; Mason, P. E.; Neilson, G. W.; Rempe, S., *submitted.*

35. Berendsen, H. J. C.; Grigera, J. R.; Straatsma, T. P., The Missing Term in Effective Pair Potentials. *J. Phys. Chem.* **1987,** *91*, 6269-6271.

36. Jorgensen, W. L.; Chandrasekhar, J.; Madura, J. D.; Impey, R. W.; Klein, M. L., Comparison of Simple Potential Functions for Simulating Liquid Water. *J. Chem. Phys.* **1983,** *79*, 926-935.

37. Hess, B.; Kutzner, C.; van der Spoel, D.; Lindahl, E., GROMACS 4: Algorithms for Highly Efficient, Load-Balanced, and Scalable Molecular Simulation. *J. Chem. Theor. Comput.* **2008,** *4*, 435-447.

38. Bussi, G.; Donadio, D.; Parrinello, M., Canonical Sampling through Velocity Rescaling. *J. Chem. Phys.* **2007,** *126*, 014101.

39. Miyamoto, S.; Kollman, P. A., SETTLE - An Analytical Version of the Shake and Rattle Algorithm for Rigid Water Models. *J. Comput. Chem.* **1992,** *13*, 952-962.

40. Essmann, U.; Perera, L.; Berkowitz, M. L.; Darden, T.; Lee, H.; Pedersen, L. G., A Smooth Particle Mesh Ewald Method. *J. Chem. Phys.* **1995,** *103*, 8577-8593.

41. Mason, P. E.; Dempsey, C. E.; Neilson, G. W.; Kline, S. R.; Brady, J. W., Preferential Interactions of Guanidinum Ions with Aromatic Groups over Aliphatic Groups. *J. Am. Chem. Soc.* **2009,** *131*, 16689-16696.

42. Mason, P. E.; Neilson, G. W.; Enderby, J. E.; Saboungi, M. L.; Dempsey, C. E.; MacKerell, A. D.; Brady, J. W., The Structure of Aqueous Guanidinium Chloride Solutions. *J. Am. Chem. Soc.* **2004,** *126*, 11462-11470.

43. Bowron, D. T.; Soper, A. K.; Finney, J. L., Temperature Dependence of the Structure of a 0.06 mole Fraction Tertiary Butanol-Water Solution. *J. Chem. Phys.* **2001,** *114*, 6203-6219.

44. Mason, P. E.; Heyda, J.; Fischer, H. E.; Jungwirth, P., Specific Interactions of Ammonium Functionalities in Amino Acids with Aqueous Fluoride and Iodide. *J. Phys. Chem. B* **2010,** *114*, 13853-13860.

45. Mason, P. E.; Neilson, G. W.; Enderby, J. E.; Saboungi, M. L.; Brady, J. W., Neutron Diffraction and Computer Simulation Studies of D-xylose. *J. Am. Chem. Soc.* **2005,** *127*, 10991-10998.

46. Chialvo, A. A.; Simonson, J. M., Solvation and Ion Pair Association in Aqueous Metal Sulfates: Interpretation of NDIS Raw Data by Isobaric-Isothermal Molecular Dynamics Simulation. *Coll. Czechoslovak Chem. Commun.* **2010,** *75*, 405-424.

47. Humphrey, W.; Dalke, A.; Schulten, K., VMD: Visual Molecular Dynamics. *J. Mol. Graph.* **1996,** *14*, 33-38.